Available online at http://scik.org
Commun. Math. Biol. Neurosci. 2026, 2026:49
https://doi.org/10.28919/cmbn/9743
ISSN: 2052-2541

SEMI-ANALYTICAL TREATMENT OF FUZZY RISK DIABETES MODEL IN OMAN

A. F. JAMEEL[1,*], E. B. BASHIER[1], A. K. ALOMARI[2], WALID WANNES[1,3], KHAMIS AL KALBANI[1]
[1]Mathematics Education Program, Faculty of Education and Arts, Sohar University, Sohar 311, Oman,
[2]Department of Mathematics, Faculty of Science, Islamic University of Madinah, 42351, Madinah, Saudi Arabia,
[3]Faculty of Sciences of Sfax, Department of Mathematics, Soukra road km 3.5, B.P. 1171, 3000, Sfax, Tunisia

Abstract: Diabetes mellitus is a growing public health concern in Oman, with rising prevalence linked to lifestyle changes and genetic factors. Effective risk prediction models are essential for early intervention and management. In the interim, the semi-analytical approaches may offer simpler solutions without requiring large-scale numerical calculations or linearization and discretization techniques which could be difficult to use with fuzzy differential equation models. This study proposes a semi-analytical approach to develop a robust diabetes risk model tailored to the Omani population. By integrating clinical, demographic, and biochemical variables, the model employs a combination of analytical techniques to enhance predictive accuracy while maintaining interpretability. Additionally, solving the fuzzy differential equations, a semi-analytical method is employed, combining analytical techniques with numerical approximations to handle the inherent fuzziness in the system. This approach ensures robust and interpretable solutions while accounting for imprecise data common in medical studies. The model is validated using real-world clinical data from Oman, demonstrating its effectiveness in predicting diabetes risk trends under different scenarios. The proposed solution offers a scalable tool for policymakers and healthcare providers to implement targeted prevention strategies, potentially reducing the diabetes burden in Oman. The results highlight the flexibility of the FDE-based model in addressing uncertainty, providing healthcare policymakers with a valuable tool for early intervention strategies.

---

[*]Corresponding author
E-mail address: AJassar@su.edu.om
Received December 18, 2025

Keywords: fuzzy differential equations; diabetes model; semi-analytical method; mathematical modeling in epidemiology.

2020 AMS Subject Classification: 34A07, 92C50.

1. INTRODUCTION

have gained popularity in a number of fields, such as learning theory, linguistics, automata, decision-making, pattern categorization, algorithms, and mathematical modeling. Due to numerous applications in physics, applied sciences, biology, and engineering, fuzzy differential equations (FDEs) have unquestionably become an indispensable tool for modeling a variety of everyday occurrences as well as potential uncertainties [1]. Real-world understanding of the development of unitizing epidemiological biological problems has been greatly aided by mathematical models [2]. However, mathematical modeling of diabetes that involves system of ordinary differential equations is a complex process that involves capturing the physiological, metabolic, and behavioral factors influencing blood glucose dynamics [3]. The impact of these factors varies between individuals due to biological heterogeneity, lifestyle differences, and disease progression such as physiological & metabolic, Pharmacokinetic & Pharmacodynamic, behavioral lifestyle and disease progression & comorbidities [4]. Therefore, the appearance of system FDEs model for diabetes models, incorporating uncertainty in parameters through fuzzy numbers. utilized to analyze the behavior of phenomena that are subject to imprecise or uncertain factors. Thus, it is crucial to examine the solution of FDEs models in applications, particularly when the parameters are uncertain and cannot be estimated using the commonly used techniques. In such cases, using FDEs is a logical way to represent dynamic systems with embedded uncertainty. Unlike numerical approaches, this type of approach has the flexibility to give approximate and exact solutions to both linear and nonlinear problems without any requirement for discretization and linearization and provide a simple way to ensure the convergence of solution series including fuzzy diabetes models [1,5]. Those fuzzy models' solutions will be shown as a series of polynomial functions. This will make it easier to show the convergence solution's degree through graphical representation. The well-known standard variational iteration technique (VIM) has been discovered to be one of the approaches that may guarantee the convergence of solutions in FDEs [6-9]. Comparing this approach to other semi-analytical techniques such as the homotopy perturbation method (HPM) and the Adomian decomposition method (ADM), less computing work is needed [10,11]. Meanwhile, Multistage Variational Iteration Method (MVIM) is an extension of the standard VIM that divides the domain into multiple subintervals (stages) and applies VIM sequentially over each subinterval [12]. It found that the series solution of some mathematical models via MVIM computed step-by-step over small intervals, improving accuracy for long-time simulations and handling abrupt changes in fuzzy parameters or initial conditions [13]. The use of MVIM and VIM to solve fuzzy models in the form of system of initial value problems is limited which involves HIV infection model [13,14] but in recent years MVIM used in serval applications of differential equations in crisp biological models [15,16]. According to [17-22], because the high-risk population is a major reservoir for future diabetes cases, the prevalence of diabetes in Oman is expected to rise in the upcoming years. Consequently, it's intriguing to create a model that uses FDEs and simulates the model data using a new MVIM extension. This work's innovation is divided into two stages. The first involves creating a fuzzy differential equation model for diabetes risk dynamics in Oman (FRD) and using fuzzy sets theory techniques to incorporate ambiguity in the model parameters in the form of fuzzy numbers. In phase two, the produced model's numerical outputs are simulated by analyzing the standard VIM to obtain a new form of MVIM. It is crucial to remember that many basic fuzzy definitions, claims, and ideas that are not included in this work are well known. As demonstrated in references [19-23], the concepts pertaining to fuzzy level sets, fuzzy numbers and associated operations, fuzzy functions, fuzzy Zadeh extension theory, integration of fuzzy functions, and fuzzy initial value problems are easily accessible in previous research.

2. ANALYSIS OF FUZZY RISK MODEL DIABETES

On the basis of [1,2], we construct the FRD model as a linear system of fuzzy initial value problems, which can be found in the form below.

$$\begin{cases} \frac{d\tilde{X}(t)}{dt} = \tilde{a}\tilde{X}(t) + \tilde{b}\tilde{Y}(t) - \tilde{c}\tilde{X}(t) - \tilde{\mu}\tilde{X}(t) \\ \frac{d\tilde{Y}(t)}{dt} = \tilde{w}(P - \tilde{X}(t) - \tilde{Y}(t)) - \tilde{b}\tilde{Y}(t) - \tilde{\mu}\tilde{Y}(t) \end{cases} \quad (1)$$

Subject to fuzzy initial conditions

$$\tilde{X}(0) = \tilde{X}_0, \tilde{Y}(0) = \tilde{Y}_0$$

In this model (1), $\tilde{X}(t)$ is a fuzzy variable represents population with diabetes in Oman, $\tilde{Y}(t)$ is a fuzzy variable represents population at high risk of developing diabetes in Oman, while the change of these populations is in the form of fuzzy Hukuhara derivative where P is the total population of Oman. The fuzzy parameters in (1) are described in Table 1 as follows:

Table 1. Notation of the fuzzy parameters corresponding to model (1)

Fuzzy parameter	Parameter description
$\tilde{a}$	Incidence rate of diabetes
$\tilde{b}$	Progression rate from high risk to diabetes per year
$\tilde{c}$	Rate of diagnosis and treatment
$\tilde{w}$	Rate of developing high risk factors
$\tilde{\mu}$	Natural mortality rate

According to the fuzzy analysis in [14], the following defuzzification are defined as follows for all fuzzy level sets $r \in [0,1]$:

$$\frac{d\tilde{X}(t;r)}{dt} = \begin{cases} \frac{d\underline{X}(t;r)}{dt} \\ \frac{d\overline{X}(t;r)}{dt} \end{cases} \quad (2)$$

$$\frac{d\tilde{X}(t;r)}{dt} = \begin{cases} \frac{d\underline{Y}(t;r)}{dt} \\ \frac{d\overline{Y}(t;r)}{dt} \end{cases} \quad (3)$$

where $\tilde{X}(t;r) = [\underline{X}(t;r), \overline{X}(t;r)]$ and $\tilde{Y}(t;r) = [\underline{Y}(t;r), \overline{Y}(t;r)]$. Also, the fuzzy parameters of model (1) can be defined as bellow:

$$\begin{cases} [\tilde{a}]_r = [\underline{a}, \overline{a}]_r \\ [\tilde{b}]_r = [\underline{b}, \overline{b}]_r \\ [\tilde{c}]_r = [\underline{c}, \overline{c}]_r \\ [\tilde{w}]_r = [\underline{w}, \overline{w}]_r \\ [\tilde{\mu}]_r = [\underline{\mu}, \overline{\mu}]_r \end{cases} \quad (4)$$

where the fuzzy initial conditions are $\tilde{X}(0;r)=[\underline{X}(0;r),\overline{X}(0;r)]$ and $\tilde{Y}(0;r)=[\underline{Y}(0;r),\overline{Y}(0;r)]$, such that the initial values are $[\tilde{X}_0]_r=[\underline{X}_0,\overline{X}_0]_r$ and $[\tilde{Y}_0]_r=[\underline{Y}_0,\overline{Y}_0]_r$. Applying Eqs (2-4), the model (1) can be identified as the lower and upper bound of FRD model followed the properties of fuzzy Hukuhara derivative such that

$$\begin{cases} \frac{d\underline{X}(t;r)}{dt} = [\underline{a}]_r\underline{X}(t;r) + [\underline{b}]_r\underline{Y}(t;r) \\ \quad - [\underline{c}]_r\underline{X}(t;r) - [\underline{\mu}]_r\underline{X}(t;r) \\ \frac{d\underline{Y}(t;r)}{dt} = [\underline{w}]_r\left(N-\underline{X}(t;r)-\underline{Y}(t;r)\right) \\ \quad - [\underline{b}]_r\underline{Y}(t;r) - [\underline{\mu}]_r\underline{Y}(t;r) \\ \underline{X}(0;r) = [\underline{X}_0]_r, \underline{Y}(0;r) = [\underline{Y}_0]_r \end{cases} \tag{5}$$

$$\begin{cases} \frac{d\overline{X}(t;r)}{dt} = [\overline{a}]_r\overline{X}(t;r) + [\overline{b}]_r\overline{Y}(t;r) \\ \quad - [\overline{c}]_r\overline{X}(t;r) - [\overline{\mu}]_r\overline{X}(t;r) \\ \frac{d\overline{Y}(t;r)}{dt} = [\overline{w}]_r\left(N-\overline{X}(t;r)-\overline{Y}(t;r)\right) \\ \quad - [\overline{b}]_r\overline{Y}(t;r) - [\overline{\mu}]_r\overline{Y}(t;r) \\ \overline{X}(0;r) = [\overline{X}_0]_r, \overline{Y}(0;r) = [\overline{Y}_0]_r \end{cases} \tag{6}$$

3. Fuzzy Multistage Method Development

The fundamental analysis of VIM in a fuzzy environment, which was taken from [13], is utilized in the development of fuzzy MVIM, which is designed to be compatible with the FRD model. As stated in [14], the system of fuzzy differential equations for any fuzzy level set r on the interval [0,1] is presented as follows:

$$\tilde{D}_i[\tilde{q}_i(t;r)] + \tilde{N}_i[\tilde{q}_i(t;r)] = \tilde{G}_i(t;r) \text{ for } i,\dots,m \tag{7}$$

where $\tilde{D}_i=\frac{\partial}{\partial t}$ is first order fuzzy H-derivatives considered as the linear operators of Eq. (7) in terms crisp variable represent the time t, $\tilde{N}_i$ is a nonlinear operators involving linear and nonlinear terms of the fuzzy variable $\tilde{q}_i(t;r)$. Also, $\tilde{G}_i(t;r)$ denoted as fuzzy inhomogeneous terms of Eq. (7). According to analysis in section 2, Eq. (7) defuzzification by using these concepts leads as to the following forms.

$$\begin{cases}[\underline{D_i}]_r \underline{q_i}(t;r)+[\underline{N_i}]_r \underline{q_i}(t;r)=\underline{G_i}(t;r)\\ [\overline{D}_i]_r \overline{q}_i(t;r)+[\overline{N}_i]_r \overline{q}_i(t;r)=\overline{G}_i(t;r)\end{cases} \tag{8}$$

such that

$\tilde{q}_i(t;r)=\left[\underline{q_i}(t;r),\overline{q}_i(t;r)\right]$,

$\widetilde{D}_i(t;r)=\left[\frac{\partial \underline{D_i}(t;r)}{\partial t},\frac{\overline{D}_i(t;r)}{\partial t}\right]$,

$\widetilde{N}_i(t;r)=\left[\underline{N_i}(t;r),\overline{N}_i(t;r)\right]$,

$\tilde{G}_i(t;r)=\left[\underline{G_i}(t;r),\overline{G}_i(t;r)\right]$.

The FVIM form is shown by the following formula, which is based on VIM in [12]. Eq. (7) can be stated as follows:

$$\tilde{q}_{i,n+1}(t;r)=\tilde{q}_{i,n}(t;r)+\int_0^t \lambda_i\{\widetilde{D}_i\tilde{q}_{i,n}(s;r)+\widetilde{N}_i\tilde{q}_{i,n}(s;r)-\tilde{G}_i(s;r)\}ds \tag{9}$$

From variational theory [30]. the optimal solution of Eq. (7) relay on the Lagrange multiplier $\tilde{\lambda}_i$, $\widetilde{N}_i\tilde{q}_{i,n}(t;r)$ is considered as restricted variation, in the other word $\delta\widetilde{N}_i\tilde{q}_{i,n}(t;r)=0$. Eqs. (7) describe the aforementioned correction functional, and [29] states that the stationary condition of this equation can drive the generic Lagrange form as follows.

$$\tilde{\lambda}_i(s)=\frac{(-1)^m}{(m-1)!}(s-t)^{m-1} \tag{10}$$

where m is order of the fuzzy differential equation. Now the final formulation of the fuzzy MVIM corresponding with FRD model (1) has the following system iteration:

$$\begin{cases}\tilde{X}_{j+1}(t;r)=\tilde{X}_j(t;r)-\int_0^t\left(\frac{d\tilde{X}_j(s;r)}{ds}-[\tilde{a}]_r\tilde{X}_j(s;r)-[\tilde{b}]_r\tilde{Y}_j(s;r)+[\tilde{c}]_r\tilde{X}_j(s;r)+[\tilde{\mu}]_r\tilde{X}_j(s;r)\right)ds\\ \tilde{Y}_{j+1}(t;r)=\tilde{Y}_j(t;r)-\int_0^t\left(\frac{d\tilde{Y}_j(s;r)}{ds}-[\tilde{w}]_r\left(P-\tilde{X}_j(s;r)-\tilde{Y}_j(s;r)\right)+[\tilde{b}]_r\tilde{Y}_j(s;r)+[\tilde{\mu}]_r\tilde{Y}_j(s;r)\right)ds\end{cases} \tag{11}$$

From the analysis in Section 2 and the fuzzy Hukuhara derivative, the fuzzy solution of model (1) via MVIM can be written as follows

Lower bound solution

$$\begin{cases}\underline{X}_{j+1}(t;r)=\underline{X}_j(t;r)-\int_0^t\left(\frac{d\underline{X}_j(s;r)}{ds}-[\underline{a}]_r\underline{X}_j(s;r)-[\underline{b}]_r\underline{Y}_j(s;r)+[\underline{c}]_r\underline{X}_j(s;r)+[\underline{\mu}]_r\underline{X}_j(s;r)\right)ds\\ \underline{Y}_{j+1}(t;r)=\underline{Y}_j(t;r)-\int_0^t\left(\frac{d\underline{Y}_j(s;r)}{ds}-[\underline{w}]_r\left(P-\underline{X}_j(s;r)-\underline{Y}_j(s;r)\right)+[\underline{b}]_r\underline{Y}_j(s;r)+[\underline{\mu}]_r\underline{Y}_j(s;r)\right)ds\\ \underline{X}(t;r)=[\underline{X_0}]_r,\underline{Y}(t;r)=[\underline{Y_0}]_r\end{cases} \tag{12}$$

Upper bound solution

$$\begin{cases}\overline{X}_{j+1}(t;r)=\overline{X}_j(t;r)-\int_0^t\left(\frac{d\overline{X}_j(s;r)}{ds}-[\overline{a}]_r\overline{X}_j(s;r)-\left[\overline{b}\right]_r\overline{Y}_j(s;r)+[\overline{c}]_r\overline{X}_j(s;r)+[\overline{\mu}]_r\,\overline{X}_j(s;r)\right)ds\\ \overline{Y}_{j+1}(t;r)=\overline{Y}_j(t;r)-\int_0^t\left(\frac{d\underline{Y}_j(s;r)}{ds}-[\overline{w}]_r\left(P-\overline{X}_j(s;r)-\overline{Y}_j(s;r)\right)+\left[\overline{b}\right]_r\overline{Y}_j(s;r)+[\overline{\mu}]_r\,\overline{Y}_j(s;r)\right)ds\\ \overline{X}(t;r)=\left[\overline{X}_0\right]_r,\overline{Y}(t;r)=\left[\overline{Y}_0\right]_r\end{cases}\quad(13)$$

where $t\in[\ 0,T]$ and $j=1,2,3,\ldots$ such that the MVIM solution of Eqs (12-13) converge according to [19]. Next step is to divide the time interval of the problem into a sequence of small-time intervals and solving them separately. This approach allows for more accurate and reliable solutions for long time span, as it takes into account the complex dynamical behaviours of the proposed model. By considering approximate solution of model in a sequence of intervals, $[t_0=0,t_1)$, $[t_1,t_2)$, $[t_2,t_3)$,…, $[t_{k-1},t_k=T]$, $k=1,2,\ldots$. Then Eqs (12-13) can solve via VIM for each subinterval, using the solution from the previous interval as an initial approximation for the next interval until reaches the final subinterval to obtain the improved Eqs. (12-13). According to [2], The fuzzy MVIM formulas of Eqs (12-13) are given by:

$$\begin{cases}\underline{X}_{j+1}(t;r)=\underline{X}_j(t;r)-\int_0^t\left(\frac{d\underline{X}_j(s;r)}{ds}-\left[\underline{a}\right]_r\underline{X}_j(s;r)-\left[\underline{b}\right]_r\underline{Y}_j(s;r)+\left[\underline{c}\right]_r\underline{X}_j(s;r)+\left[\underline{\mu}\right]_r\,\underline{X}_j(s;r)\right)ds\\ \underline{Y}_{j+1}(t;r)=\underline{Y}_j(t;r)-\int_0^t\left(\frac{d\underline{Y}_j(s;r)}{ds}-\left[\underline{w}\right]_r\left(P-\underline{X}_j(s;r)-\underline{Y}_j(s;r)\right)+\left[\underline{b}\right]_r\underline{Y}_j(s;r)+\left[\underline{\mu}\right]_r\,\underline{Y}_j(s;r)\right)ds\\ \underline{X}(t;r)=\underline{X}(0;r)=z_1^*,\underline{Y}(t;r)=\underline{Y}(0;r)=z_2^*\end{cases}\quad(14)$$

$$\begin{cases}\overline{X}_{j+1}(t;r)=\overline{X}_j(t;r)-\int_0^t\left(\frac{d\overline{X}_j(s;r)}{ds}-[\overline{a}]_r\overline{X}_j(s;r)-\left[\overline{b}\right]_r\overline{Y}_j(s;r)+[\overline{c}]_r\overline{X}_j(s;r)+[\overline{\mu}]_r\,\overline{X}_j(s;r)\right)ds\\ \overline{Y}_{j+1}(t;r)=\overline{Y}_j(t;r)-\int_0^t\left(\frac{d\underline{Y}_j(s;r)}{ds}-[\overline{w}]_r\left(P-\overline{X}_j(s;r)-\overline{Y}_j(s;r)\right)+\left[\overline{b}\right]_r\overline{Y}_j(s;r)+[\overline{\mu}]_r\,\overline{Y}_j(s;r)\right)ds\\ \overline{X}(t;r)=\overline{X}(0;r)=z_3^*,\overline{Y}(t;r)=\overline{Y}(0;r)=z_4^*\end{cases}\quad(15)$$

where t^* is the left-end point of each sub intervals, and $z_1^*, z_2^*,\ z_3^*, z_4^*$ are considered as the initial approximations of Eqs. (14-15). Having the first initial conditions, one would be able to solve Eqs. (14-15) for all unknowns $\overline{X}_j(t;r),\underline{X}_j(t;r),\overline{Y}_j(t;r)$, $\underline{Y}_j(t;r)$, $j=1,2,\ldots$ In order to perform iteration in every subintervals of the same length, $[t_0,t_1)$, $[t_1,t_2)$, $[\ t_2,t_3)$,… $[\ t_{k-1},t_k]$. The values of the following need to be determined beforehand:

$$\begin{cases}\overline{X}_0^*(t,r)=\overline{X}(t^*,r),\underline{X}_0^*(t,r)=\underline{X}(t^*,r),\\ \overline{Y}_0^*(t,r)=\overline{Y}(t^*,r),\underline{Y}_0^*(t,r)=\underline{Y}(t^*,r).\end{cases}\quad(16)$$

All the initial approximations can be derived from the beginning value $t^*=t_0$. Therefore, using the earlier n-term estimates, a straightforward method for obtaining the required values may be found. $\bar{\beta}_{1,n}(t^*;r), \underline{\beta}_{2,n}(t^*;r), \underline{\beta}_{3,n}(t^*;r)$, and $\bar{\beta}_{4,n}(t^*;r)$ of the preceding subinterval such that the approximate solution of model (1) by fuzzy MVIM is as follows

$$\begin{cases} \bar{X}_0^*(t,r) = \bar{\beta}_{1,n}(t^*;r) = \lim\limits_{j\to n-1} \bar{X}_j(t;r), \\ \underline{X}_0^*(t,r) = \underline{\beta}_{2,n}(t^*;r) = \lim\limits_{j\to n-1} \underline{X}_j(t;r), \\ \bar{Y}_0^*(t,r) = \underline{\beta}_{3,n}(t^*;r) = \lim\limits_{j\to n-1} \bar{Y}_j(t;r), \\ \underline{Y}_0^*(t,r) = \bar{\beta}_{4,n}(t^*;r) = \lim\limits_{j\to n-1} \underline{Y}_j(t;r). \end{cases} \tag{17}$$

4. Model Analysis

A state in which the system does not undergo any changes is referred to as an equilibrium point in a dynamical system. In model (1), the equilibrium points convert into fuzzy sets when r belongs to the interval $[0,1]$. In other words, rather than each numeric point, as is the case with crisp models, the healthy range is defined relative to the degree of fuzzy membership functions that correspond to the fuzzy parameters and initial conditions of model (1). This ensures that the conditions of the patients converge to the equilibrium point for each fuzzy level set. To obtain the equilibrium points of model 1, redefine model one as follows:

$$\begin{cases} \frac{d\tilde{X}(t;r)}{dt} = [\tilde{\theta}]_r \tilde{X}(t;r) + [\tilde{b}]_r \tilde{Y}(t;r) \\ \frac{d\tilde{Y}(t;r)}{dt} = [\widetilde{w}]_r P - [\widetilde{w}]_r \tilde{X}(t;r) - [\tilde{\sigma}]_r \tilde{Y}(t;r) \end{cases} \tag{18}$$

where the new fuzzy parameters are $\tilde{\theta} = \tilde{a} - \tilde{c} - \tilde{\mu}$ and $\tilde{\sigma} = -(\widetilde{w} + \tilde{b} + \tilde{\mu})$. As can be seen below, the equilibrium points$(\tilde{X}_{e,r}, \tilde{Y}_{e,r})$ for each fuzzy level set $r \in [0,1]$ by setting the fuzzy derivatives of model (18) equal to zero as demonstrated in [3].

$$\begin{cases} \tilde{X}_{e,r} = \left[\frac{\widetilde{w}\tilde{b}P}{\widetilde{w}\tilde{b}+\tilde{\theta}\tilde{\sigma}}\right]_r \\ \tilde{Y}_{e,r} = \left[\frac{-\tilde{\theta}\widetilde{w}P}{\widetilde{w}\tilde{b}+\tilde{\theta}\tilde{\sigma}}\right]_r \end{cases} \tag{19}$$

Define the fuzzy linear system in the following form:

$$\frac{d}{dt}\begin{bmatrix} \tilde{X}(t;r) \\ \tilde{Y}(t;r) \end{bmatrix} = \mathrm{JO}\begin{bmatrix} \tilde{X}(t;r) \\ \tilde{Y}(t;r) \end{bmatrix} + \begin{bmatrix} 0 \\ [\widetilde{w}]_r P \end{bmatrix},$$

JO stands for the Jacobian matrix, which, in the case of a linear system, is nothing more than the coefficient matrix because:

$$\mathrm{JO} = \begin{bmatrix} [\tilde{\theta}]_r & [\tilde{b}]_r \\ -[\widetilde{w}]_r & [\tilde{\sigma}]_r \end{bmatrix} = \begin{bmatrix} [\tilde{a} - \tilde{c} - \tilde{\mu}]_r & [\tilde{b}]_r \\ -[\widetilde{w}]_r & [-(\widetilde{w} + \tilde{b} + \tilde{\mu})]_r \end{bmatrix}$$

According to the defuzzification analysis in Section 2, system (18) becomes crisp per each value $r \in [0,1]$ The eigenvalues of the JO matrix are what determine whether the equilibrium point of a linear system with dimensions of 2 rows and 2 columns is stable [5,31]. If both eigenvalues $[\tilde{\gamma}_1]_r, [\tilde{\gamma}_2]_r$ of system (18) have negative real portions, then the equilibrium is considered to be stable. According to [32], the use of the trace-determinant conditions are as follows:

$$\text{Set } \tau = \mathrm{Trace(JO)} = [\tilde{\theta} + \tilde{\sigma}]_r$$

$$\text{Set } \Lambda = |\mathrm{JO}| = [\tilde{\theta}\tilde{\sigma} + \widetilde{w}\tilde{b}]_r$$

The equilibrium is considered to be stable if $\Lambda > 0$ and $\tau < 0$ such that

$\tau = [\tilde{a} - \tilde{c} - \widetilde{w} - \tilde{b} - 2\tilde{\mu}]_r$, and

$\Lambda = [-(\tilde{a} - \tilde{c} - \tilde{\mu})(\widetilde{w} - \tilde{b} - \tilde{\mu}) + \widetilde{w}\tilde{b}]_r$.

Given that natural mortality and diagnostic rate are both stabilizing influences, it is highly probable that the condition $\tau < 0$ will remain stable. When the criterion Λ is greater than zero, it guarantees that the interaction between compartments does not result in uncontrolled development.

5. Semi Analytical Simulation

The semi-analytical simulation that was performed with MVIM and described in Section 3 will be examined in this section. This will be followed by an examination of errors and solutions to the problems that were present in the simulation. The parameters' values that are shown in Table 1 and the initial conditions of the model (1), which are displayed in Table 2 below, should be configured according to the data instructions that have been provided by the World Health Organization. in the year 2022 The Sultanate of Oman: A 2022 Report on the Noncommunicable Diseases of the Country Geneva: International Diabetes Federation, World Health Organization, 2025. The International Diabetes Federation's Diabetes Atlas, Eleventh Edition and, based on the data and analysis that were presented in [17-23], we are able to derive the following defuzzification of the estimated fuzzy parameter:

Table 2. The defuzzification form of the estimated Parameters of model (1)

Fuzzy parameter	Parameter estimation	Parameter defuzzification
$\tilde{X}_0$	$450000 \sim 650000$	$[450000 + 100000r, 650000 - 100000r]$
$\tilde{Y}_0$	$750000 \sim 1250000$	$[750000 + 250000r, 1250000 - 250000r]$
$\tilde{a}$	$1\% \sim 2\%$	$[0.01 + 0.015r, 0.02 - 0.015r]$
$\tilde{b}$	$5\% \sim 12\%$	$[0.05 + 0.03r, 0.12 - 0.04r]$
$\tilde{c}$	$70\% \sim 95\%$	$[0.7 + 0.15r, 0.95 - 0.1r]$
$\tilde{w}$	$3\% \sim 8\%$	$[0.05 + 0.03r, 0.08 - 0.03r]$
$\tilde{\mu}$	$2.8\% \sim 3.8\%$	$[0.028 + 0.04r, 0.038 - 0.06r]$

From the above parameters in Table 2, model (1) can rewrite as follows:

$$\begin{cases} \frac{d\overline{X}(t;r)}{dt} = (0.01 + 0.015\mathrm{r})\underline{X}(t;r) + (0.05 + 0.03\mathrm{r})\underline{Y}(t;r) - (0.7 + 0.15\mathrm{r})\underline{X}(t;r) \\ \qquad -(0.028 + 0.04\mathrm{r})\underline{X}(t;r) \\ \frac{d\underline{Y}(t;r)}{dt} = (0.05 + 0.03\mathrm{r})\left(P - \underline{X}(t;r) - \underline{Y}(t;r)\right) - (0.05 + 0.03\mathrm{r})\underline{Y}(t;r) \\ \qquad -(0.028 + 0.04\mathrm{r})\underline{Y}(t;r) \\ \underline{X}(0;r) = 450000 + 100000\mathrm{r}, \underline{Y}(0;r) = 750000 + 250000\mathrm{r} \end{cases} \tag{20}$$

$$\begin{cases} \frac{d\overline{X}(t;r)}{dt} = (0.02 - 0.015\mathrm{r})\overline{X}(t;r) + (0.12 - 0.04\mathrm{r})\overline{Y}(t;r) - (0.95 - 0.1\mathrm{r})\overline{X}(t;r) \\ \qquad -(0.038 - 0.06\mathrm{r})\overline{X}(t;r) \\ \frac{d\overline{Y}(t;r)}{dt} = (0.08 - 0.03\mathrm{r})\left(P - \overline{X}(t;r) - \overline{Y}(t;r)\right) - (0.12 - 0.04\mathrm{r})\overline{Y}(t;r) \\ \qquad -(0.038 - 0.06\mathrm{r})\overline{Y}(t;r) \\ \overline{X}(0;r) = 650000 - 100000\mathrm{r}, \overline{Y}(0;r) = 1250000 - 250000\mathrm{r} \end{cases} \tag{21}$$

where Oman's population is $P = 5357663$, according to the National Center for Statistics and Information (NCSI) of Oman. The next step is to analyze Eq. (20-21) on the new MVIM that is described in Section 3 to simulate model (1) from different values of fuzzy level set. Additionally, an error analysis is defined in terms of accuracy of MVIM approximate solution via residual error as follows:

$$\begin{cases} RE_x = \frac{d\sum_{i=0}^{n}\tilde{X}_i(t;r)}{dt} - \tilde{a}\sum_{i=0}^{n}\tilde{X}_i(t;r) - \tilde{b}\sum_{i=0}^{n}\tilde{Y}_i(t;r) + \tilde{c}\sum_{i=0}^{n}\tilde{X}_i(t;r) + \tilde{\mu}\sum_{i=0}^{n}\tilde{X}_i(t;r) \\ RE_y = \frac{d\sum_{i=0}^{n}\tilde{Y}_i(t;r)}{dt} - \tilde{w}\left(P - \sum_{i=0}^{n}\tilde{X}_i(t;r) - \sum_{i=0}^{n}\tilde{Y}_i(t;r)\right) + \tilde{b}\sum_{i=0}^{n}\tilde{Y}_i(t;r) + \tilde{\mu}\sum_{i=0}^{n}\tilde{Y}_i(t;r) \end{cases}$$

where $\sum_{i=0}^{n}\tilde{X}_i(t;r)$ and $\sum_{i=0}^{n}\tilde{Y}_i(t;r)$ represent the fuzzy MVIM series solution of model (1) that can be summarized in Figures 1-12 as follows:

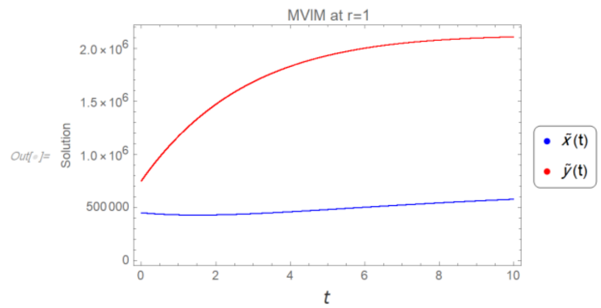

(a)

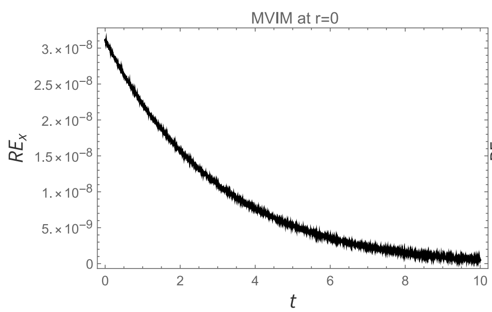

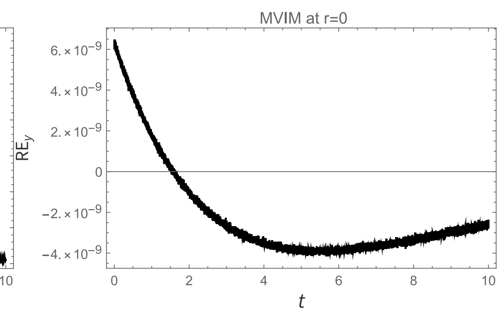

(b) (c)

Fig 1. Lower Solution and accuracy of MIVM for Eq. (19) at $r = 0$ for ten years $t = 10$.

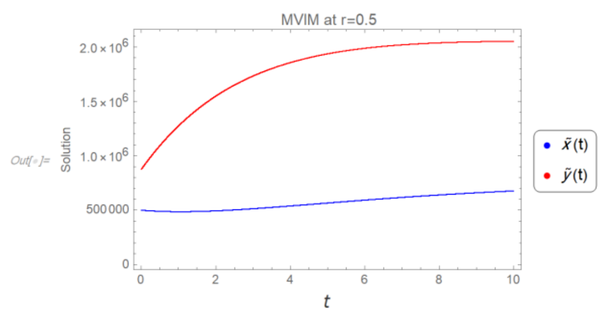

(a)

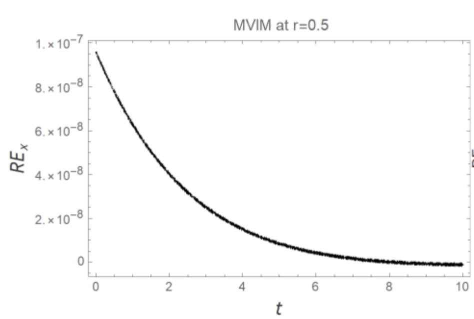

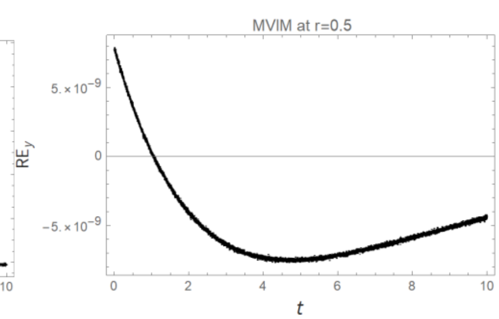

(b) (c)

Fig 2. Lower Solution and accuracy of MIVM for Eq. (19) at $r = 0.5$ for ten years $t = 10$.

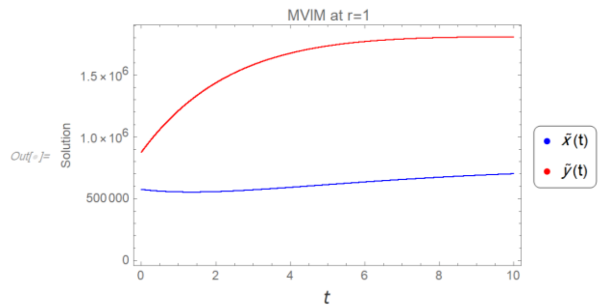

(a)

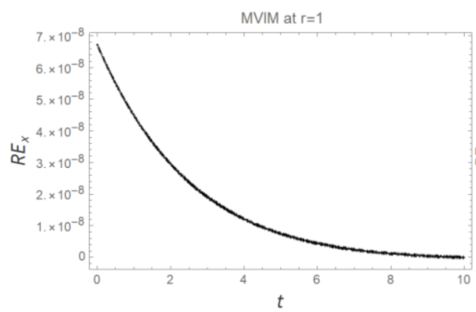

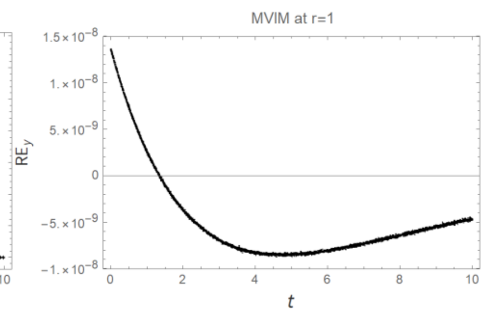

(b) (c)

Fig 3. Lower Solution and accuracy of MIVM for Eq. (19) at $r = 1$ for ten years $t = 10$.

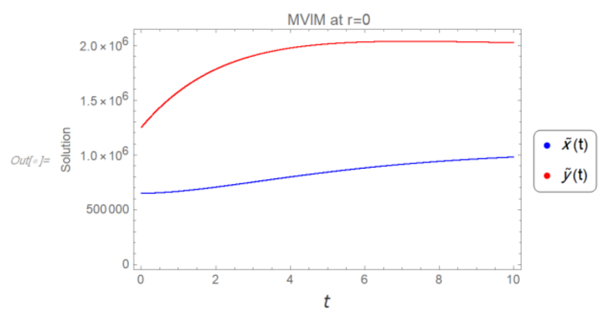

(a)

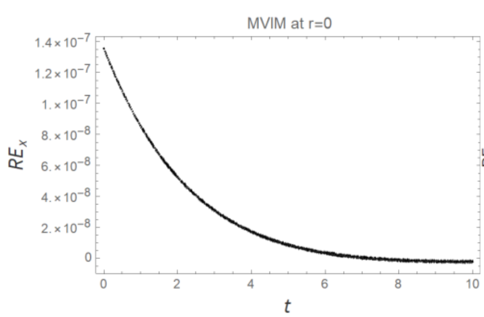

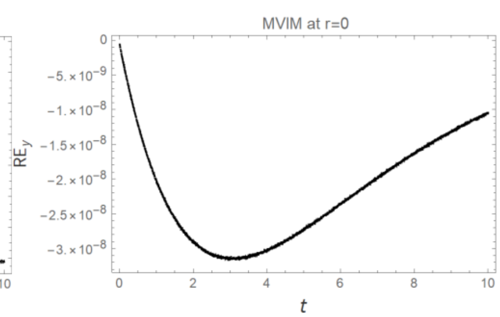

(b) (c)

Fig 4. Upper Solution and accuracy of MIVM for Eq. (20) at $r = 0$ for ten years $t = 10$.

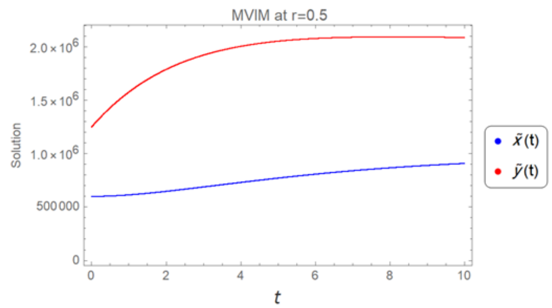

(a)

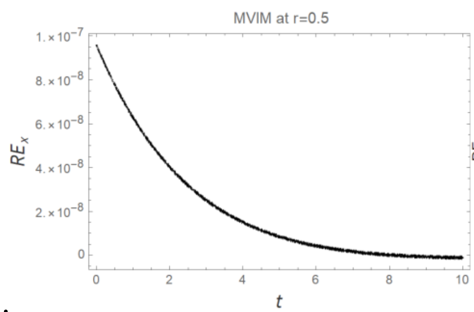

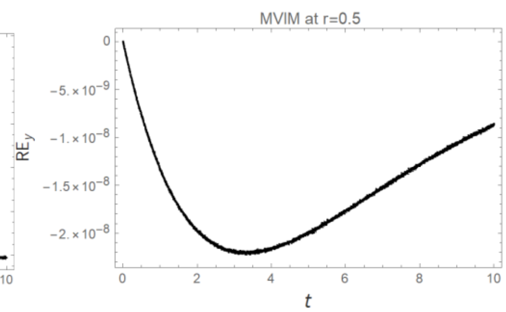

(b) (c)

Fig 5. Upper Solution and accuracy of MIVM for Eq. (20) at $r = 0.5$ for ten years $t = 10$.

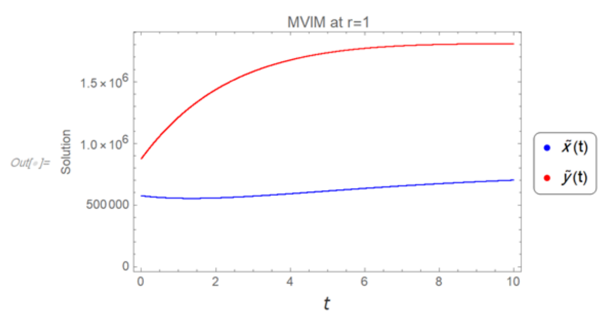

(a)

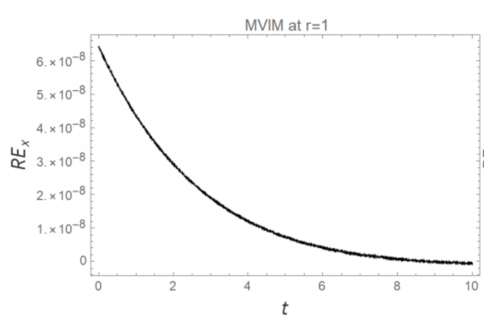

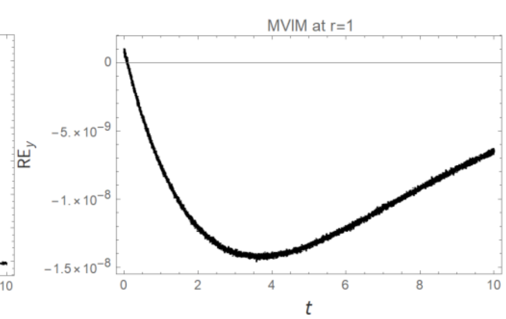

(b) (c)

Fig 6. Upper Solution and accuracy of MIVM for Eq. (19) at $r = 1$ for ten years $t = 10$.

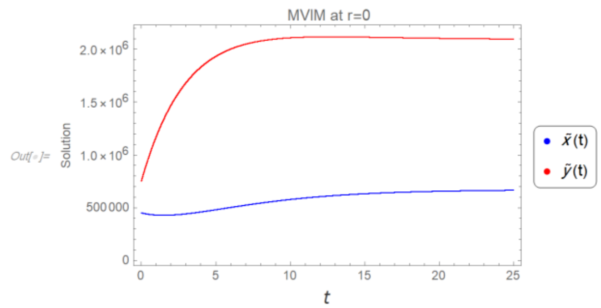

(a)

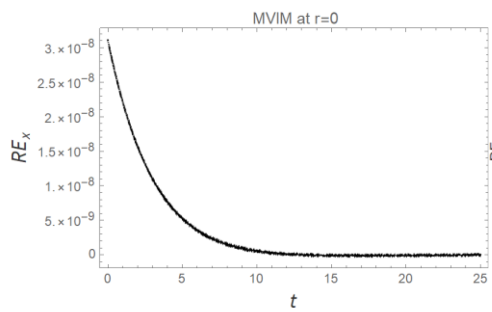

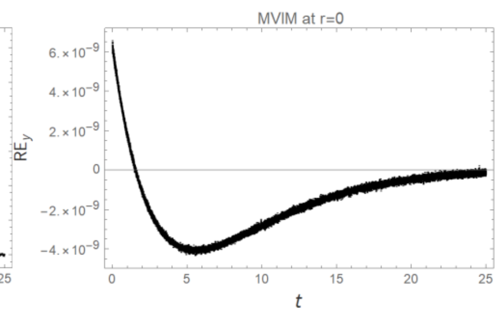

(b) (c)

Fig 7. Lower Solution and accuracy of MIVM for Eq. (19) at $r = 0$ for 25 years $t = 25$.

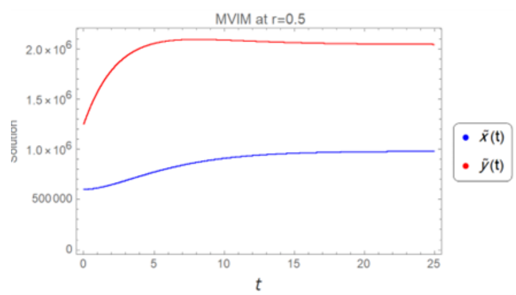

(a)

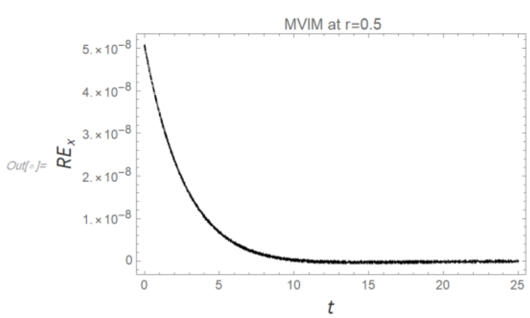

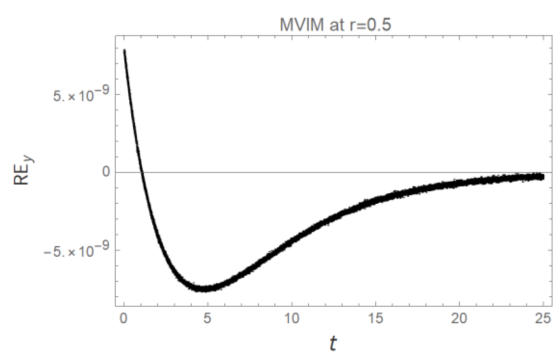

(b) (c)

Fig 8. Lower Solution and accuracy of MIVM for Eq. (20) at $r = 0.5$ for 25 years $t = 25$.

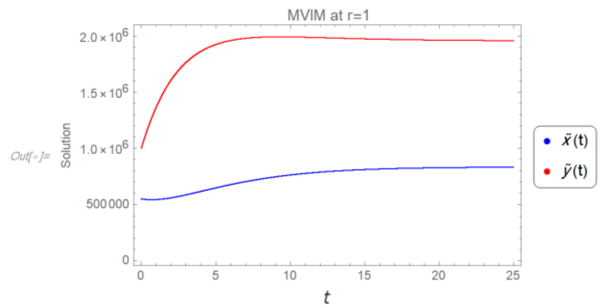

(a)

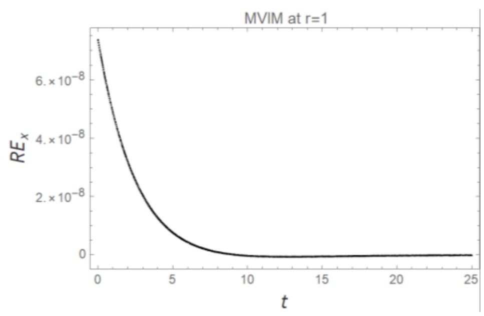

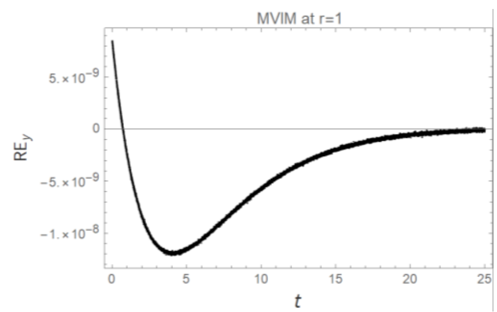

(b) (c)

Fig 9. Lower Solution and accuracy of MIVM for Eq. (20) at $r = 1$ for 25 years $t = 25$.

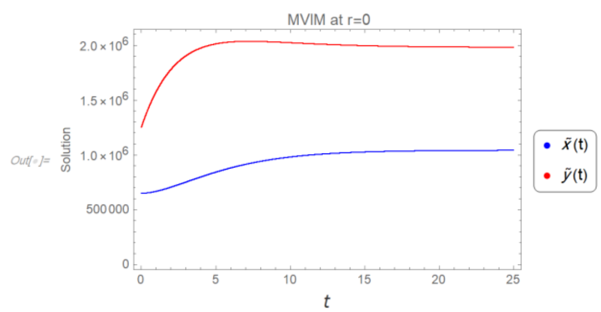

(a)

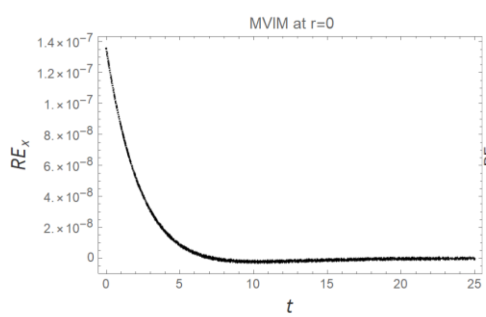

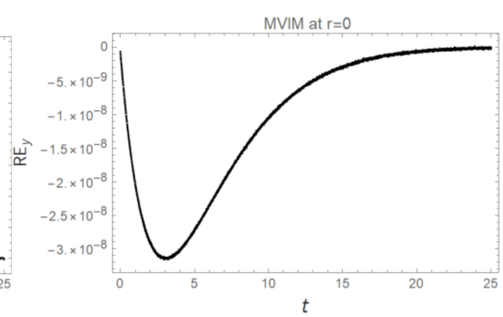

(b) (c)

Fig 10. Upper Solution and accuracy of MIVM for Eq. (20) at $r = 0$ for 25 years $t = 25$.

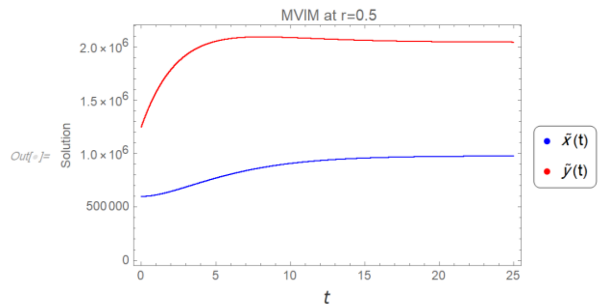

(a)

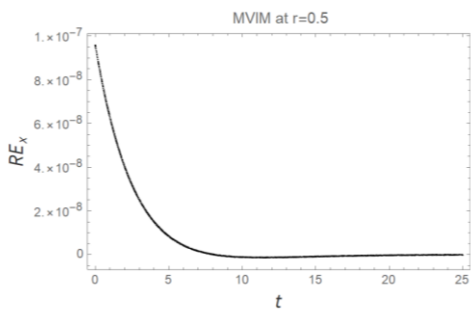

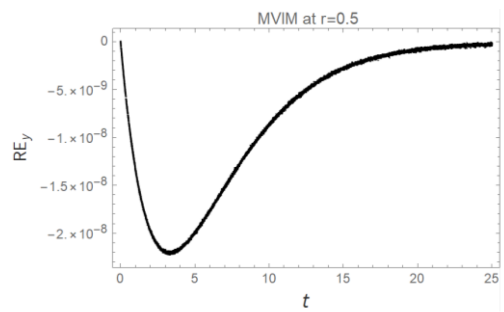

(b) (c)

Fig 11. Upper Solution and accuracy of MIVM for Eq. (20) at $r = 0.5$ for 25 years $t = 25$.

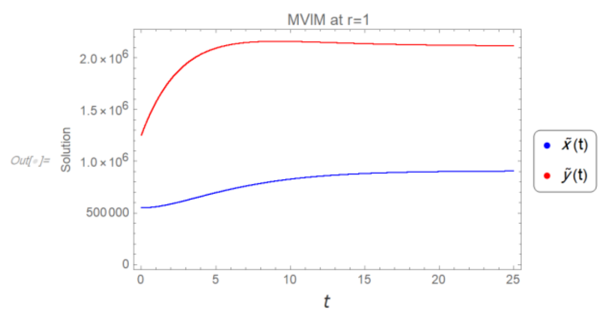

(a)

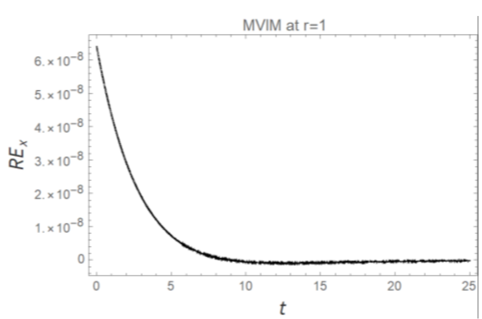

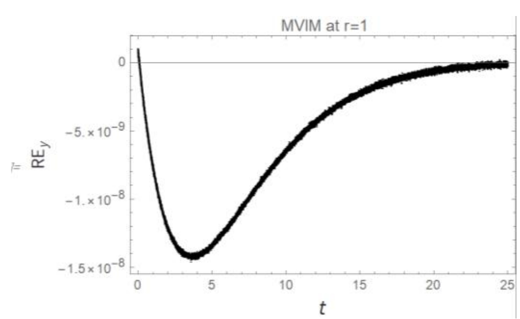

(b) (c)

Fig 12. Upper Solution and accuracy of MIVM for Eq. (20) at $r = 1$ for 25 years $t = 25$.

From Eq. (19) the equilibrium points at $r = 0$ for Eq. (20) is $\left(\underline{X}_{e,0}, \underline{Y}_{e,0}\right) = (145510.77, 2{,}089334.66)$. According to Section 4 when $r = 0$ the Jacobian matrix can be defined as bellow:

$$\mathrm{JO} = \begin{bmatrix} -0.718 & 0.05 \\ -0.05 & -0.128 \end{bmatrix}, \tau = -0.846 \text{ and } \Lambda = 0.094404 > 0.$$

Consequently, both eigenvalues of the matrix possess negative real components, indicating that the equilibrium is a stable node. In the asymptotically stable equilibrium, the solutions converge to $\left(\underline{X}_{e,0}, \underline{Y}_{e,0}\right)$ as the equilibrium is reached in the case of $t \rightarrow \infty$. At $t = 10$ years, it is likely Eq. (20) is still in the transient phase if its initial conditions are distant from equilibrium such that at $r = 0$:

$\underline{X}(0; r) = 450000 > \underline{X}_{e,0}, \underline{Y}(0; r) = 750000 < \underline{Y}_{e,0}$. Initially, there was not even close to equilibrium. Additionally, the eigenvalues of JO matrix at $r = 0$ of Eq. (19) is -0.132 and -0.71375, such that the slowest decay rate $e^{-0.123}$influences the long-term. The time constant is approximate $\frac{1}{0.132} \approx 7.5$ years. After a period of ten years, the proportion of original displacement that is still present is about $e^{-1.23} \approx 0.267$. This indicates that approximately 26.7% of the initial errors is still present along the slow eigenvector direction. For $t = 25$ years $e^{-3.3} \approx 0.0.0367$, then only 3.7% is left, which is substantially closer to $\left(\underline{X}_{e,0}, \underline{Y}_{e,0}\right)$. Therefore, Eq. (20) is more stable within time $t = 25$ at $r = 0$ as stated if Figures 1(a)-7(a). In the same manner, the stability of Equation (20) at $r = 0.5$ is depicted as shown in the following illustration:

The equilibrium point is approximately is $\left(\underline{X}_{e,0.5}, \underline{Y}_{e,0.5}\right) = (157280.36,\ 1948504.76)$

$\mathrm{JO} = \begin{bmatrix} -0.8055 & 0.065 \\ -0.065 & -0.178 \end{bmatrix}$, $\tau = -0.9835$ and $\Lambda = 0.37685625 > 0$. Then equilibrium $\left(\underline{X}_{e,0.5}, \underline{Y}_{e,0.5}\right)$is asymptotically stable since the eigenvalues of JO is $(-0.184798, -0.798702)$. for $r = 0.5$:

$$\underline{X}(0; r) = 500000 > \underline{X}_{e,0.5}, \underline{Y}(0; r) = 875000 < \underline{Y}_{e,0.5}$$

The greater eigenvalue, which is less negative, is the one that determines the rate. The time constant is approximate $\frac{-1}{-0.184798} \approx 5.42$ years. So, by $t = 10$ years $e^{-1.84798} \approx 0.16$, Eq. (20) is closed to $\left(\underline{X}_{e,0.5}, \underline{Y}_{e,0.5}\right)$. For $t = 25$ years $e^{-4.62} \approx 0.0099$, Eq. (20) is essentially at $\left(\underline{X}_{e,0.5}, \underline{Y}_{e,0.5}\right)$. Therefore, the system is stable since both of its eigenvalues are negative; after ten years, it is somewhat close to equilibrium, and after twenty-five years, it is quite close to equilibrium as displayed in Figures 2(a) and 8(a). To finish the analysis for the lower bound solution via three teams of MVIM for model (1) linked to Eq. (20) we check the stability at $r = 1$ such that:

The equilibrium point is approximately is $\left(\underline{X}_{e,1}, \underline{Y}_{e,1}\right) = (1.67465 \times 10^5,\ 1.86868 \times 10^6)$

$\mathrm{JO} = \begin{bmatrix} -0.893 & 0.08 \\ -0.08 & -0.228 \end{bmatrix}$, $\tau = -1.121$ and $\Lambda = 0.210004 > 0$. Then equilibrium $\left(\underline{X}_{e,1}, \underline{Y}_{e,1}\right)$is asymptotically stable since the eigenvalues of JO is $(-0.237767, -0.883233)$. for $r = 1$:

$$\underline{X}(0; r) = 600000 > \underline{X}_{e,1}, \underline{Y}(0; r) = 1000000 < \underline{Y}_{e,1}$$

The greater eigenvalue, which is less negative, is the one that determines the rate. The time constant is approximate $\frac{-1}{-0.237767} \approx 4.20$ years. So, by $t = 10$ years $e^{-2.37767} \approx 0.093$, Eq. (20) is closed to $\left(\underline{X}_{e,1}, \underline{Y}_{e,1}\right)$. For $t = 25$ years $e^{-4.62} \approx 0.00262106$, Eq. (20) is essentially at $\left(\underline{X}_{e,1}, \underline{Y}_{e,1}\right)$. Consequently, the system exhibits stability as both eigenvalues are negative; after 10 years, it approaches equilibrium, and after twenty-five years, it is significantly near equilibrium, as illustrated in Figures 3(a) and 9(a). Now, for the upper bound solution of model (1) corresponding to Eq. (21) is started when $r = 0$:

The equilibrium point is approximately is $\left(\overline{X}_{e,0}, \overline{Y}_{e,0}\right) = (219795.9,\ 1773399.7)$

$\mathrm{JO} = \begin{bmatrix} -0.968 & 0.12 \\ -0.08 & -0.238 \end{bmatrix}$, $\tau = -1.206 < 0$ and $\Lambda = 0.239984 > 0$. Then equilibrium $\left(\overline{X}_{e,0}, \overline{Y}_{e,0}\right)$is asymptotically stable since the eigenvalues of JO is $(-0.2514, -0.9546)$. for $r = 0$:

$$\overline{X}(0; r) = 650000 > \overline{X}_{e,0}, \overline{Y}(0; r) = 1250000 < \overline{Y}_{e,0}$$

The greater eigenvalue, which is less negative, is the one that determines the rate. The time constant is approximate $\frac{-1}{-0.2514} \approx 3.98$ years. So, by $t = 10$ years $e^{-2.514} \approx 0.081$, Eq. (20) is closed to $\left(\overline{X}_{e,0}, \overline{Y}_{e,0}\right)$. For $t = 25$ years $e^{-6.28} \approx 0.0019$, Eq. (20) is essentially at $\left(\overline{X}_{e,0}, \overline{Y}_{e,0}\right)$.

Consequently, the system exhibits stability as both eigenvalues are negative; after 10 years, it approaches equilibrium, and after twenty-five years, it is significantly near equilibrium, as illustrated in Figures 4(a) and 10(a). For $r = 0.5$

The equilibrium point is approximately is $\left(\overline{X}_{e,0.5}, \overline{Y}_{e,0.5}\right) = (221257.25, 1981355.79)$

$\mathrm{JO} = \begin{bmatrix} -0.8955 & 0.10 \\ -0.065 & -0.173 \end{bmatrix}$, $\tau = -1.206 < 0$ and $\Lambda = 0.1614215 > 0$. Then equilibrium $\left(\overline{X}_{e,0.5}, \overline{Y}_{e,0.5}\right)$is asymptotically stable since the eigenvalues of JO is $(-0.182118, -0.886381)$. for $r = 0.5$:

$$\overline{X}(0;r) = 600000 > \overline{X}_{e,0.5}, \overline{Y}(0;r) = 1.125 \times 10^{6} < \overline{Y}_{e,0.5}$$

The greater eigenvalue, which is less negative, is the one that determines the rate. The time constant is approximate $\frac{-1}{-0.182118} \approx 5.49$ years. So, by $t = 10$ years $e^{-1.82118} \approx 0.162$, Approximately 16% of the initial disruption persists

of Eq. (20) is closed to $\left(\overline{X}_{e,0.5}, \overline{Y}_{e,0.5}\right)$. For $t = 25$ years $e^{-4.55} \approx 0.0106$, Eq. (20) is essentially very close to $\left(\overline{X}_{e,0.5}, \overline{Y}_{e,0.5}\right)$. Consequently, the system exhibits stability as both eigenvalues are negative; after 10 years, it approaches equilibrium, and after twenty-five years, it is significantly near equilibrium, as illustrated in Figures 5(a) and 11(a). Finally, at $r = 1$:

The equilibrium point is approximately is $\left(\overline{X}_{e,1}, \overline{Y}_{e,1}\right) = (236637, 2434560$

$\mathrm{JO} = \begin{bmatrix} -0.823 & 0.08 \\ -0.05 & -0.108 \end{bmatrix}$, $\tau = -0.931 < 0$ and $\Lambda = 0.092884 > 0$. Then equilibrium $\left(\overline{X}_{e,1}, \overline{Y}_{e,1}\right)$is asymptotically stable since the eigenvalues of JO is $(-0.113639, -0.817361)$. for $r = 1$:

$$\overline{X}(0;r) = 550000 > \overline{X}_{e,1}, \overline{Y}(0;r) = 1000000 < \overline{Y}_{e,1}$$

The greater eigenvalue, which is less negative, is the one that determines the rate. The time constant is approximate 8.8 years. So, by $t = 10$ years $e^{-1.13639} \approx 0.321$, Approximately 32% of the initial disruption persists of Eq. (20) is closed to $\left(\overline{X}_{e,1}, \overline{Y}_{e,1}\right)$. For $t = 25$ years $e^{-2.840975} \approx 0.058$, Eq. (20) is essentially very close to $\left(\overline{X}_{e,1}, \overline{Y}_{e,1}\right)$. Consequently, the system exhibits stability as both eigenvalues are negative; after 10 years, it approaches equilibrium, and after twenty-five years, it is significantly near equilibrium, as illustrated in Figures 6(a) and 12(a). With only three terms of the new MVIM series solution, it is evident that the semi-analytical solution of model (1) is stable as a case study with time increasing, as validated by pictures 1 (b-c) to Figure 12 (b-c). This is evident from the analysis that was presented above. The fuzzy system presented in Eq. (20-21) possesses a distinct stable equilibrium for each r, with the convergence is more rapid for $r = 1$ than for $r = 0$ and $r = 0.5$. Moreover, at $r = 0.5$, Eq. (20) and Eq. (21) are relatively proximate in $\tilde{X}$, but exhibit greater variability in $\tilde{Y}$. The ranges indicate considerable uncertainty regarding the long-term at-risk population $\tilde{Y}$, whereas the diabetic population $\tilde{X}$ is more reliably constrained. In general, the convergence rate indicates that the spectral abscissa becomes increasingly negative as r grows from 0 to 1 in the lower bound system. In the framework of Oman's diabetic model, this indicates that the uncertainty band (attributable to fuzzy parameters) diminishes over the long term, allowing the system to consistently converge on these equilibrium populations irrespective of initial conditions within the specified fuzzy range. Public health planning may utilize equilibrium values as long-term forecasts.

6. Synopsis and Findings

The study presented two developed phases; a new model is developed in the form of the FIVIs system to utilize the diabetes cases in terms of vague parameters in Oman. A new exaltation of VIM is developed to be fuzzy in terms of simulation and utilization of the proposed model, followed by model analysis in terms of stability analysis. The new extension of MFVIM demonstrates improved performance by generating polynomial functions that visually illustrate the easy convergence of the series solution. The conclusion that was reached was that when the MFVIM was combined with just a few terms, it exhibited enhanced results over an extended period of time while maintaining a high degree of accuracy. Additionally, the proposed simulated model concluded that it is stable for all fuzzy level sets that correlate with the fuzzy parameter, as well as for the semi-analytical solution obtained by MVIM. Overall, for Oman's diabetes model, this study band indicates that there is uncertainty in the populations at risk of developing diabetes and those who already have the disease in the long term as a result of ambiguity in the parameters, but the system always stabilizes. These bands can be utilized for scenario planning in the context of public health planning. The study demonstrates the capability and precision of the new MFVIM in solving fuzzy models, suggesting its potential as an effective technique for tackling other types of fuzzy models, including fractional and nonlinear models, within chaotic systems in future applications.

ACKNOWLEDGEMENTS

The authors gratefully acknowledge the financial support provided by the Ministry of Higher Education, Research and Innovation Authority (RIA), Oman, through the Block Funding Program at Sohar University (SU Ref: SU/BFP/RG/2024/15). This support was essential for the successful completion of this research.

CONFLICT OF INTERESTS

The authors declare that there is no conflict of interests.

REFERENCES

[1] K.H. Gazi, A. Biswas, P. Singh, M. Rahaman, S. Maity, A. Mahata, S.P. Mondal, A Comprehensive Literature Review of Fuzzy Differential Equations with Applications, J. Fuzzy Ext. Appl. 6 (2025), 134-161. https://doi.org/10.22105/jfea.2024.449970.1426.

[2] M. Routaray, P.K. Sahu, D.N. Chalishajar, The Fuzzy Differential Transform Method for the Solution of the System of Fuzzy Integro-Differential Equations Arising in Biological Model, Mathematics 11 (2023), 3840. https://doi.org/10.3390/math11183840.

[3] A. Mahata, S.P. Mondal, S. Alam, B. Roy, Mathematical Model of Glucose-Insulin Regulatory System on Diabetes Mellitus in Fuzzy and Crisp Environment, Ecol. Genet. Genom. 2 (2017), 25-34. https://doi.org/10.1016/j.egg.2016.10.002.

[4] P. Vinothini, K. Kavitha, A Review on Fuzzy Mathematical Modeling in Biology, Adv. Math.: Sci. J. 9 (2020), 5987-5996. https://doi.org/10.37418/amsj.9.8.67.

[5] A. Acharya, A. Mahata, M. Karak, N. Sil, S. Mukherjee, et al., Stability Analysis of Diabetes Mellitus Model in Neutrosophic Fuzzy Environment, Frankl. Open 8 (2024), 100144. https://doi.org/10.1016/j.fraope.2024.100144.

[6] A.F. Jameel, H.H. Saleh, A. Azmi, A. Alomari, N.R. Anakira, et al., Efficient Approximate Analytical Methods for Nonlinear Fuzzy Boundary Value Problem, Int. J. Electr. Comput. Eng. 12 (2022), 1916. https://doi.org/10.11591/ijece.v12i2.pp1916-1928.

[7] N.R. Anakira, A.H. Shather, A.F. Jameel, A.K. Alomari, A. Saaban, Direct Solution of Uncertain Bratu Initial Value Problem, Int. J. Electr. Comput. Eng. 9 (2019), 5075. https://doi.org/10.11591/ijece.v9i6.pp5075-5083.

[8] H.H. Saleh, A. A., A.F. Jameel, Approximation Treatment for Linear Fuzzy HIV Infection Model by Variational Iteration Method, Math. Stat. 9 (2021), 342-349. https://doi.org/10.13189/ms.2021.090316.

[9] H. Jafari, M. Saeidy, D. Baleanu, The Variational Iteration Method for Solving N-Th Order Fuzzy Differential Equations, Open Phys. 10 (2011), 76-85. https://doi.org/10.2478/s11534-011-0083-7.

[10] A.F. Jameel, S.G. Amen, A. Saaban, N.H. Man, F.M. Alipiah, Homotopy Perturbation Method for Solving Linear Fuzzy Delay Differential Equations Using Double Parametric Approach, Math. Stat. 8 (2020), 551-558. https://doi.org/10.13189/ms.2020.080508.

[11] M. Osman, Z. Gong, A.M. Mustafa, Comparison of Fuzzy Adomian Decomposition Method with Fuzzy VIM for Solving Fuzzy Heat-Like and Wave-Like Equations with Variable Coefficients, Adv. Differ. Equ. 2020 (2020), 327. https://doi.org/10.1186/s13662-020-02784-w.

[12] Y. Rangkuti, A. Alomari, N. Anakira, A. Jameel, Approximate-Analytic Solution of Hyperchaotic Finance System by Multistage Approach, Sains Malays. 51 (2022), 1905-1914. https://doi.org/10.17576/jsm-2022-5106-25.

[13] H.H. Saleh, A. Azmi, A.F. Jameel, Computational Solution and Analysis of Fuzzy Nonlinear HIV Infection Model via New Multistage Fuzzy Variational Iteration Method, Math. Stat. 12 (2024), 219-228. https://doi.org/10.13189/ms.2024.120301.

[14] H.H. Saleh, A. A., A.F. Jameel, Approximation Treatment for Linear Fuzzy HIV Infection Model by Variational Iteration Method, Math. Stat. 9 (2021), 342-349. https://doi.org/10.13189/ms.2021.090316.

[15] I.N. Khasanah, A. Suryanto, U. Habibah, Multistage Variational Iteration Method for a SEIQR COVID-19 Epidemic Model with Isolation Class, Commun. Math. Biol. Neurosci. 2022 (2022), 27. https://doi.org/10.28919/cmbn/7236.

[16] I. Hassan, A.O. Collins, I.O. Obiajulu, The Revised New Iterative Method for Solving the Model Describing Biological Species Living Together, Amer. J. Comput. Appl. Math. 6 (2016), 136-143.

[17] A. Al-Mawali, A. Al-Harrasi, S.K. Jayapal, M. Morsi, A.D. Pinto, et al., Prevalence and Risk Factors of Diabetes in a Large Community-Based Study in the Sultanate of Oman: STEPS Survey 2017, BMC Endocr. Disord. 21 (2021), 42. https://doi.org/10.1186/s12902-020-00655-9.

[18] E.K. Hoogeveen, The Epidemiology of Diabetic Kidney Disease, Kidney Dial. 2 (2022), 433-442. https://doi.org/10.3390/kidneydial2030038.

[19] S. Al Amri, J. Singh, L. Al Balushi, T. Al Ghafri, M.N. Al Balushi, et al., Prevalence and Associated Factors of Diabetes Mellitus Type 2 among Tuberculosis Patients in Muscat, Oman, 2017–2020, Oman Med. J. 38 (2023), e526. https://doi.org/10.5001/omj.2023.82.

[20] N.A. Al-Lawati, H. Alfonso, J. Al-Lawati, Development and Validation of a Risk Score for Diabetes Screening in Oman, Oman Med. J. 37 (2022), e340. https://doi.org/10.5001/omj.2021.123.

[21] H. Al Thiabat, S. Elbanna, M. Quadier, M. Dayyeh, B. Abunnadi, et al., Clinical Presentation and Outcomes of Diabetic Ketoacidosis in Pediatric and Adolescent Patients at a Tertiary Hospital in Jordan, Front. Pediatr. 13 (2025), 1635037. https://doi.org/10.3389/fped.2025.1635037.

[22] A. Alareeki, S.F. Awad, A. Al-Mawali, M. Morsi, J.A. Critchley, et al., Impact of Mitigating Obesity, Smoking, and Physical Inactivity on Type 2 Diabetes Mellitus Burden in Oman: Insights from Mathematical Modeling, BMJ Open Diabetes Res. Care 12 (2024), e004248. https://doi.org/10.1136/bmjdrc-2024-004248.

[23] A. Al-Mawali, S.K. Jayapal, M. Morsi, W. Al-Shekaili, A.D. Pinto, et al., Prevalence of Risk Factors of Non-Communicable Diseases in the Sultanate of Oman: STEPS Survey 2017, PLOS ONE 16 (2021), e0259239. https://doi.org/10.1371/journal.pone.0259239.

[24] S. Bodjanova, Median Alpha-Levels of a Fuzzy Number, Fuzzy Sets Syst. 157 (2006), 879-891. https://doi.org/10.1016/j.fss.2005.10.015.

[25] M. Mizukoshi, L. Barros, Y. Chalco-Cano, H. Román-Flores, R. Bassanezi, Fuzzy Differential Equations and the Extension Principle, Inf. Sci. 177 (2007), 3627-3635. https://doi.org/10.1016/j.ins.2007.02.039.

[26] L.C. de Barros, F. Santo Pedro, Fuzzy Differential Equations with Interactive Derivative, Fuzzy Sets Syst. 309 (2017), 64-80. https://doi.org/10.1016/j.fss.2016.04.002.

[27] S. Abbasbandy, T. Viranloo, Ó. López-Pouso, J. Nieto, Numerical Methods Forfuzzy Differential Inclusions, Comput. Math. Appl. 48 (2004), 1633-1641. https://doi.org/10.1016/j.camwa.2004.03.009.

[28] Z. John, F. S. Fadhel, S. Ariffin Abdul Karim, T. Yuan Ying, Stabilizability and Solvability of Fuzzy Reaction-Diffusion Equation Using Modified Backstepping Control Method for Matrix Differential Equation, Malays. J. Fundam. Appl. Sci. 21 (2025), 2159-2173. https://doi.org/10.11113/mjfas.v21n3.4249.

[29] M. Rafei, H. Daniali, D. Ganji, Variational Iteration Method for Solving the Epidemic Model and the Prey and Predator Problem, Appl. Math. Comput. 186 (2007), 1701-1709. https://doi.org/10.1016/j.amc.2006.08.077.

[30] J. He, Variational Iteration Method—Some Recent Results and New Interpretations, J. Comput. Appl. Math. 207 (2007), 3-17. https://doi.org/10.1016/j.cam.2006.07.009.

[31] C. Kolodziej, R. Priemer, Stability Analysis of Fuzzy Systems, J. Frankl. Inst. 336 (1999), 851-873. https://doi.org/10.1016/S0016-0032(99)00009-5.

[32] Y. Zhu, Stability Analysis of Fuzzy Linear Differential Equations, Fuzzy Optim. Decis. Mak. 9 (2010), 169-186. https://doi.org/10.1007/s10700-010-9080-3.